Neutral Beam Power Measurements Inside the ASDEX Torus

Yü Zengliang*, A. Stäbler, O. Vollmer

IPP 4/208 November 1982

MAX-PLANCK-INSTITUT FÜR PLASMAPHYSIK

8046 GARCHING BEI MÜNCHEN

MAX-PLANCK-INSTITUT FÜR PLASMAPHYSIK

GARCHING BEI MÜNCHEN

Neutral Beam Power Measurements Inside the ASDEX Torus

Yü Zengliang*, A. Stäbler, O. Vollmer

IPP 4/208 November 1982

* On leave from the Academia Sinica, Peking
The Peoples' Republic of China

Die nachstehende Arbeit wurde im Rahmen des Vertrages zwischen dem Max-Planck-Institut für Plasmaphysik und der Europäischen Atomgemeinschaft über die Zusammenarbeit auf dem Gebiete der Plasmaphysik durchgeführt.

IPP 4/208

Neutral Beam Power Measurements Inside the ASDEX Torus

Yü Zengliang*
A. Stäbler
O. Vollmer

November 1982

Abstract

Neutral beam power measurements inside the ASDEX torus are done with a retractable calorimeter which is only radiation cooled. The calorimeter plate made from Molybdenum is subdivided into nine segments whose increase in energy content due to a shot yields the absorbed beam power. Different models for the backward extrapolation of the measured temperature curves are examined for a series of low energy shots with the result that pure radiation cooling is a valid assumption. Furthermore, a temperature correction to the measured power is derived from these experiments. The evaluation of the shots onto this calorimeter is done by a computer program. The application of this program to a few full power shots shows that a neutral power up to 3.2 MW has been injected into the ASDEX vessel by the two injectors with an overall efficiency of up to 40%. Reionization losses due to the ASDEX stray field are less than 10%; they do not show any dependence upon the pulse length for shots up to 200 ms.

* On leave from the Academia Sinica, Peking
The Peoples' Republic of China

C O N T E N T S

		Page
I.	Introduction	1
II.	Description of the Torus Calorimeter	1
III.	Determination of the Beam Power	3
	III.1 Evaluation of the Thermocouple Signals	3
	III.2 Temperature Correction	6
	III.3 The Evaluation Program	7
IV.	Full Power Shots onto the Torus Calorimeter	8
V.	Summary	9
	Acknowledgements	10
	Appendix A	10
	References	14
	Figures	15

I. INTRODUCTION

The analysis of neutral beam heated plasmas requires the knowledge of the neutral power provided to the plasma as an important input parameter. It is therefore necessary to measure the beam power injected into the vacuum vessel of the plasma machine. This power may deviate from the power determined inside the neutral beam line for two reasons: on the one hand, the aperture of the duct which connects the injector with the plasma vessel restricts geometrically the beam transmission, on the other hand, the finite background pressure within this duct causes reionization processes which result in a further reduction of the net power hitting the plasma surface. It has been suggested that the latter process may even cause severe losses of power ("beam choking") /1,2/.

The ASDEX neutral beam injection system /3/ is equipped with a retractable calorimeter inside the ASDEX torus (torus calorimeter). This allows to determine the neutral power transmitted through the duct in shots synchronized with actual ASDEX discharges. The design of this torus calorimeter together with the appropriate data acquisition are briefly described in Section II. The various problems associated with the evaluation of the measured signals are reported in Section III. By applying different theoretical assumptions to the experimental results of a series of low energy shots onto the calorimeter a final version of the evaluation program is derived. This program is then used to evaluate a few full power shots (Section IV). A brief summary is given in Section V.

II. DESCRIPTION OF THE TORUS CALORIMETER

On the ASDEX tokamak the neutral beam power is delivered by two beam lines both injecting tangentially into the plasma. It is, therefore, impossible to rely on inner wall armor plates for calorimetric purposes. For each beam line a movable calorimeter plate had to be fitted within the rather restricted space between the exit of the neutral beam duct and the plasma surface. Each plate is fixed onto a horizontal axis of rotation. A rota-

tion angle of about 90^0 is necessary to move the calorimeter from its "parking" position to its "in beam" position.

The plates were designed to withstand a maximum power density of $3.60 kW/cm^2$ for pulse lengths of around 200 ms; they should be cooled only by radiation. The plate material was chosen to be Molybdenum. In order to prevent high-Z material from reaching the plasma, a stainless steel back plate shields the Mo-plate against the plasma. In its "in beam" position the beam axis intersects the calorimeter plate under an angle of 40^0. Due to the individual adjustment of the four ion sources which are mounted on one beam line, the power profile at the exit of the duct is approximately elliptic with a vertical elongation /4/. Together with the angle between the beam axis and the plate this results in a nearly circular power deposition on the calorimeter. It was therefore decided to subdivide the Mo-plate into nine segments: a central plate (r = 8.7 cm) is surrounded by two concentric rings each of which is subdivided into four equal quarters of a ring. This segmentation considerably reduces the heat equilibration time inside the plate. The nine segments do not touch each other; they are fixed individually to the stainless steel back plate in a way to minimize heat conduction to this plate. The thickness of the Mo-segments is 7 mm (inner plate, first ring) and 5 mm (outer ring), respectively. The overall diameter of the calorimeter is 45 cm. It covers the total cross section of the transmitted beam. The layout of the calorimeter is illustrated in Fig. 1.

Each Mo-segment is equipped with one thermocouple. In order to reduce perturbations on the thermocouple signals and to provide the necessary isolation, the voltage signals are converted into frequency signals which are transfered via isolation transformers to the control room some 80 m away, where the data are fed to a microcomputer (MINC 11, DEC) /5/. The temperatures obtained from each of the thermocouples are sampled with a rate of one point per six seconds over a period of 10 minutes. The data are stored on a floppy disc. In parallel it is possible to give the signals via frequency to voltage conversion to a recorder.

III. DETERMINATION OF THE BEAM POWER

III.1 EVALUATION OF THE THERMOCOUPLE SIGNALS

The principle of beam power measurement is based on determinating the increase in energy content due to the absorbed beam power of each individual Mo-segment:

$$P_b = \sum_{j=1}^{9} c_{Mo}\, m_j\, (T_j - T_{j,in}) \,/\, \tau_p \qquad \text{(III.1)}$$

Here, c_{Mo} denotes the heat capacity of Molybdenum, the m_j are the masses of the different segments, τ_p is the pulse length of the shot and the $T_{j,in}$ are the temperatures of the segments before the shot. The T_j - values stand for the (hypothetic) equilibrium temperature of a segment just after the shot, assuming an instantaneous temperature equilibration within a segment. The summation has to be done over all nine segments of the calorimeter.

The main difficulty comes from the determination of the equilibrium temperatures T_j. They have to be obtained by a backward extrapolation of the measured temperature curve. The temperature equilibration via heat diffusion, however, can be estimated to be some 50 seconds. This rather long time interval requires a careful consideration of the extrapolation procedures.

A hot Mo-plate may loose energy by radiation and by heat conduction via its support structure to the back plate. Assuming that the hot plate may be described by one temperature T, the temperature evolution is given by

$$\varepsilon\, A\, \sigma\, (T^4 - T_0^4)\, dt + \lambda\, \frac{A_0}{L_0}\, (T - T_0)\, dt = - c_{Mo}\, m\, dT \qquad \text{(III.2)}$$

where A is the surface of the plate, A_0 being a representative cross section and L_0 a representative length to describe the heat conduction.

T_0 is the ambient temperature. In principle, the material constants ε (emissivity), λ (heat conductivity) and c_{Mo} are (weakly) temperature dependent which will be neglected in solving equ. III.2. The effect of this temperature dependence is, however, included in the experimental determination of an overall temperature correction described further down in this paper.

Assuming that heat conduction is the dominant cooling process, the solution of equ. III.2 is of the form

$$\ln \left(T - T_0 \right) = c_1 t + c_0 \qquad \text{(III.3)}$$

where c_0 is the integration constant determined by the initial conditions and c_1 contains the constants λ, (A_0/L_0), c_{Mo} and m.

If, on the other hand, radiation dominates the temperature development of the plate, the solution of equ. III.2 is

$$\ln \left(\frac{T - T_0}{T + T_0} \right) - 2 \operatorname{arctg} \left(\frac{T}{T_0} \right) = c_1' t + c_0' \qquad \text{(III.4)}$$

Again, c_0' is the integration constant and c_1' contains ε, A, σ, c_{Mo} and m.

If both processes equally contribute to the temperature decrease of the plate, the solution of equ. III.2, which is derived in Appendix A, may be expressed as follows:

$$\alpha \ln (T - T_0) + \beta \ln (T - L) + \frac{\gamma}{2} \ln (T^2 + aT + b)$$

$$+ \left(\delta - \frac{\gamma a}{2} \right) \frac{2}{\sqrt{4b - a^2}} \operatorname{arctg} \left(\frac{a + 2T}{\sqrt{4b - a^2}} \right) = c_1'' t + c_0'' \qquad \text{(III.5)}$$

where α, β, γ and δ are solutions of a linear equation system resulting from the decomposition to partial fractions, L is the solution

of a cubic equation in T, $a = T + L$ and $b = - R / L$ where R contains T_0 , λ , A_0 / L_0 , σ , A and ε . A more detailed definition of all these constants in equ. III.5 can be found in the Appendix A.

The common feature of all three cases is that the solution is of the form

$$f (T) = c_1 t + c_0 \qquad \text{(III.6)}$$

The constants c_0 and c_1 are determined by calculating $f (T)$ according to one of the equations III.3, III.4 or III.5 from the measured temperature values in a time interval, where the heat is equally distributed within the segments of the plate and by then applying a least square fit procedure to the pairs of (f (T), t) numbers. Backward extrapolation to $t = 0$, which is defined by the end of the shot, means that one is interested in the solution of

$$f (T_j) - c_0 = 0 \qquad \text{(III.7)}$$

for the temperature curve of the plate. This is straightforward in the case of equ. III.3. In the case of equation III.4 or III.5, the value of T_j which fulfills the implicit function (equ. III.7) is determined numerically.

The T_j - values obtained for each segment in one of the different ways, outlined above, can then be used to calculate the total beam power absorbed by the calorimeter according to equ. III.1. It should be mentioned that $f(T)$ for pure heat conduction as well as for pure radiation does not depend upon λ , (A_0 / L_0) , A or ε . Therefore, no assumptions upon those values have to be made in order to determine P_b . In the case of equ. III.5, however, $f(T)$ depends on the constants of equ. III.2 which, therefore, have to be specified when P_b is determined this way.

An example for the application of the three different extrapolation methods is illustrated in Fig. 2. Shot No. 8785 belongs to a series of low energy

shots which are described in detail further down. In evaluating this shot the time interval which is used for the least square fit was varied from 80 - 600 s to 300 - 600 s. Curve No. 1 in Fig. 2 was obtained by applying equ. III.2, i.e. assuming pure heat conduction cooling. It can be seen that the calculated beam power depends on the chosen interval, indicating that the above assumption is not correct. On the other hand, the results using the extrapolations according to equ. III.4 and III.5 (curve No. 2 and 3) are independent of the fit interval. Furthermore, there is no significant difference between the power calculated from the two different methods. These general features have been found in all cases investigated so far and lead to the conclusion that radiation is the dominant process of heat loss from the Mo-plates. Therefore, in all further calculations the equilibrium temperatures of the segments are obtained using the extrapolation according to equ. III.4.

III.2 TEMPERATURE CORRECTION

Some measurements done in the early phase of the experiment have shown that the beam power recorded by the torus calorimeter depends upon its temperature, i.e., two similar shots yield different results when the first shot hits the initially cold plate and the second one is fired onto the plate which is already at a higher temperature. In order to investigate this effect in detail, a series of low energy pulses (24 kV, 10 A per source for 200 ms) were performed, where the initial temperatures just before each shot increase sucessively from room temperature to finally 645 K for the central plate and to 505 K for the segments of the first ring. The corresponding equilibrium temperatures after the shots increase from 455 K to 755 K and from 370 K to 545 K. The outer ring sees only about 5 % of the power, therefore, no temperature correction is necessary. In between these shots, the beam power was controlled by measurements with the calorimeter inside the beam line. The power recorded by the torus calorimeter (according to equ. III.4) normalized to the power measured by the beam line calorimeter decreases from 0.91 to 0.82.

From these results, it is obvious that a temperature correction has to be included to the power determination according to equ. III.1. A detailed

evaluation of the power absorbed by the different segments in this series of shots results in the following value for the temperature correction factor:

$$g_j = (1.0 + 3.4 \cdot 10^{-4} (T_j[K] - T_0[K])) \qquad \text{III.8}$$

which has to be multiplied to the power measured by each of the segments. Since equilibrium temperatures up to about 800 K have been obtained on the central plate, which absorbs more then 50 % of the total power, the temperature correction may be in the order of up to 10 %.

The main reason for the necessity of applying such a temperature correction to the calculated beam power comes from the temperature dependence of the heat capacity c_{Mo}, which was assumed to be constant so far. From the values for the heat capacity of Molybdenum listed in Ref. /6/, it can be seen that c_{Mo} may be approximated fairly well by

$$c_{Mo}(T) = c_{Mo}(T_0) \; (1.0 + 2.1 \cdot 10^{-4} (T\,[K] - T_0\,[K]))$$

in the range between 300 K and 800 K where $c_{Mo}(T_0) = 255$ J kg^{-1}K^{-1} is the value at room temperature which is used in the calculations.

A further temperature correction can be due to the fact that the power radiated from the plate in the time during heat equilibration within the plate is not described correctly by the backward extrapolation outlined above.

III.3 THE EVALUATION PROGRAM

The different aspects discussed in this section so far have been incorporated into a computer program which calculates the beam power from the data recorded from a shot onto the torus calorimeter. The program is written in BASIC and runs on the MINC computer which is also used for the data acquisition. The measured temperature curves of each segment are read from the floppy disc. Since radiation has proved to dominate

the cooling of the plate, the following calculations are based upon equ. III.4. The constants of the right hand side of this equation are determined by a least square fit in a time interval which can be chosen by the user. The equilibrium values T_j of the different segments are obtained by numerically solving equ. III.7. In a next step, the temperature correction factors g_j (equ. III.8) are calculated and then multiplied to each summand of equ. III.1. The total beam power absorbed by the calorimeter plate is finally determined by:

$$P_b = \sum_{j=1}^{9} c_{Mo}\ m_j\ g_j\ (T_j - T_{j,in}) / \tau_p \qquad \text{(III.1')}$$

The output of the program includes the initial and equilibrium temperatures of the different segments, the total beam power and the power distribution over the segments of the calorimeter. It is further possible to print out the measured temperature curves. The program allows to have in hand the complete evaluation of a shot onto the torus calorimeter a few minutes after the data acquisition is terminated.

IV. FULL POWER SHOTS ONTO THE TORUS CALORIMETER

This section will give some results for shots with full power onto the torus calorimeter which may characterize the performance of the ASDEX neutral beam heating system to some extent. Since the data acquisition of the thermocouple signals was not available from the very beginning a few results are reported also from shots whose evaluation is based only on the temperature curves obtained on the recorder.

Full power shots onto the torus calorimeter, evaluated with the program described above, were done synchronized with actual ASDEX discharges. The power values measured in those shots are, therefore, representative for the neutral beam power provided to the plasma. The maximum power obtained so far was 3.20 MW in a 200 ms pulse, where 1.57 MW were delivered by the NW-injector and 1.63 MW by the SO-injector. This power corresponds to 84 % (NW-injector) and 88 % (SO-injector) of the neutral power measured inside the beam line in similar shots. The extracted power ($U_{ex} \cdot I_{ex}$; $U_{ex} \simeq 41$ kV) in this shot was 3.88 MW and 4.02 MW, respectively, for the two

injectors. The overall efficiency, therefore, corresponds to 40 % in both cases. The power distribution within the calorimeter was found to: 56 % on the central plate, 38 % on the first ring and the remaining 6 % on the outer ring. The values for the overall efficiency and the power distribution over the plates are representative for shots with lower power, too.

Full power shots onto the torus calorimeter without any ASDEX magnetic field have been performed in former experiments where no computerized data acquisition was available. The neutral power normalized to the power on the beam line calorimeter measured in this series of experiments was about 97 %. Hence, the geometrical transmission through the duct turns out to be quite high, as it is expected from the large cross section of the duct (elliptic cross section, 39 cm * 33 cm). Subsequent measurements with the ASDEX main field being switched on, result in a reduction of the power transmission from 97 % to about 88 %. Even if the power determination obtained by this time is not too accurate, the ratio between the power values with and without the ASDEX field should not be affected too much by this inaccuracy. These results indicate that the power losses due to reionization processes between the deflection magnet and the plasma surface are less than 10 %. No significant difference has been found for pulse lengths of 100 ms and 200 ms. It is intended to repeat those measurements applying the evaluation methods outlined above.

V. SUMMARY

The retractable calorimeter inside the ASDEX torus has proved to be a useful tool to determine the neutral beam power provided to the ASDEX plasma. Due to the space restrictions and for safety reasons, the calorimeter plates are not watercooled. The power measurement relies on the determination of the increase in energy content of the plates due to the beam. It has been shown that pure radiation cooling is a reasonable assumption to determine this energy content by backward extrapolation of the measured temperature curves. Furthermore, a temperature correction for the measured power values has been obtained experimentally. All these features are included into a computer program

which delivers a complete evaluation of a shot onto the torus calorimeter.

Values for the neutral beam power up to 3.2 MW, delivered by two injectors, have been measured with this torus calorimeter so far, the overall efficiency (neutral power into the torus / extracted power) being 40 %. Reionization losses of the neutral power downstream from the magnet through the duct to the ASDEX vessel are found to be less than 10 %. There are no indications for a time dependence of these losses within the presently used 200 ms pulses. It is intended, however, to upgrade the ASDEX neutral beam system to a 10 seconds injection /7/. For this reason a more detailed investigation of the reionization problem should be done.

ACKNOWLEDGEMENTS

The authors would like to thank the ASDEX neutral injection team for maintaining and operating the beam systems.

APPENDIX A

This Appendix should sketch the way of solving equ. III.2

$$\varepsilon\, A\, \sigma(T^4 - T_0^4)\, dt + \lambda \frac{A_0}{L_0}(T - T_0)\, dt = - c_{Mo}\, m\, dT$$

and precisely define the order of calculating the various constants given in the solution (equ. III.5). The above stated equation may be written as

$$\int \{ k_1 (T^4 - T_0^4) + k_2 (T - T_0) \}^{-1} dT = c_1 t + c_0 \qquad (A.1)$$

with $k_1 = \varepsilon A \sigma$, $k_2 = \lambda (A_0/L_0)$, $c_1 = -(1/c_{Mo} m)$ and c_0 being the integration constant. The integral of equ. (A.1) will be solved by the method

of decomposition to partial fractions. The nominator of this equation may be transformed to

$$k_1(T^4 - T_0^4) + k_2(T - T_0) = k_1(T - T_0)(T^3 + T_0T^2 + T_0^2T + R) \qquad (A.2)$$

with

$$R = T_0^3 + (k_2 / k_1) \qquad (A.3)$$

If L is defined as a solution of the cubic equation in T

$$T^3 + T_0T^2 + T_0^2T + R = 0 \qquad (A.4)$$

L has the following form

$$L = \sqrt[3]{-\frac{q}{2} + \sqrt{\frac{q^2}{4} + \frac{p^3}{27}}} + \sqrt[3]{-\frac{q}{2} - \sqrt{\frac{q^2}{4} + \frac{p^3}{27}}} - \frac{T_0}{3} \qquad (A.5)$$

with

$$p = (2/3)\, T_0^2 \qquad (A.6)$$
$$q = R - (7/27)\, T_0^3$$

Equ. (A.2) may be expressed as

$$k_1(T - T_0)(T^3 + T_0T^2 + T_0^2T + R) = \qquad (A.7)$$
$$k_1(T - T_0)(T - L)(T^2 + aT + b)$$

where the values of a and b are obtained by the comparison of the coefficients from equ. (A.7):

$$a = T_0 + L \qquad (A.8)$$
$$b = -(R/L)$$

Using equ. (A.7), the integral of equ. (A.1) has the following form

$$\int \{ k_1(T^4 - T_0^4) + k_2(T - T_0) \}^{-1} \, dT = \frac{1}{k_1} \int \left(\frac{\alpha}{T-T_0} + \frac{\beta}{T-L} + \frac{\gamma T + \delta}{T^2+aT+b} \right) dT \qquad (A.9)$$

The different expressions of the right hand side in equ. (A.9) may then be simply integrated

$$\alpha \ln (T - T_0) + \beta \ln (T - L) + \frac{\gamma}{2} \ln (T^2 + aT + b) + \left(\delta - \frac{\gamma a}{2} \right) \frac{2}{\sqrt{4b-a^2}} \operatorname{arctg} \left(\frac{a + 2T}{\sqrt{4b-a^2}} \right) = c_1 t + c_0 \qquad (A.10)$$

where the values of α, β, γ and δ are determined by the following system of linear equations obtained from the comparison of coefficients in equ. (A.9)

$$\begin{aligned} \alpha + \beta + \gamma &= 0 \\ T_0\alpha + L\beta - a\gamma + \delta &= 0 \\ (b - aL)\alpha + (b-aT_0)\beta + T_0L\gamma - a\delta &= 0 \\ R\alpha + (RT_0/L)\beta + T_0L\delta &= 1 \end{aligned} \qquad (A.11)$$

Equ. (A.10) is the solution given in the equ. (III.5) in the text. The various constants in this expression may be obtained from the equations (A.3), (A.6), (A.8) and (A.11). These equations are used calculating curve No. 3 in Fig. 2.

It may easily be shown that the solution for pure radiation cooling is included in the formalism described above. Pure radiation cooling means $k_2 = 0$ and one obtains: $R = T_0^3$, $L = -T_0$, $a = 0$ and $b = T_0^2$. The solutions of the linear equation system (A.11) in this case are

$$\begin{aligned} \alpha &= 1/(4T_0^3) \\ \beta &= -1/(4T_0^3) \\ \gamma &= 0 \\ \delta &= -1/(2T_0^3) \end{aligned}$$

Substitution of these values into equ. (A.1o) results in

$$\ln\left(\frac{T - T_0}{T + T_0}\right) - 2\,\mathrm{arctg}\left(\frac{T}{T_0}\right) = c_1't + c_0'$$

which is the solution for pure radiation cooling given in the text (equ. III.4).

REFERENCES

/1/ R.S. Hemsworth, Culham Laboratory Report CLM-R 162 (1977)

/2/ L.D. Stewart et al., Proc. of the 8th Symp. on Eng. Problems of Fusion Research, San Francisco (1979), p. 844

/3/ A. Staebler et al., Proc. of the 9th Symp. on Eng. Problems of Fusion Research, Chicago (1981), p. 767

/4/ J.H. Feist et al., Proc. of the 8th Symp. on Eng. Problems of Fusion Research, San Francisco (1979), p. 1001

/5/ D. Cooper et al., Proc. of the 12th SOFT, Juelich (1982), paper E 23, to be published

/6/ Thermophysical Properties of Matter (The TPRC Data Series), Vol. 4, ed. Y.S. Touloukian, E.H. Buyco, IFI/Plenum New York-Washington 1970, p.135

/7/ Application for Euratom Preferential Support for ASDEX Long Pulse Injection, EUR-FU/SP81/59/2 (March, 82), Brussels (Belgium)

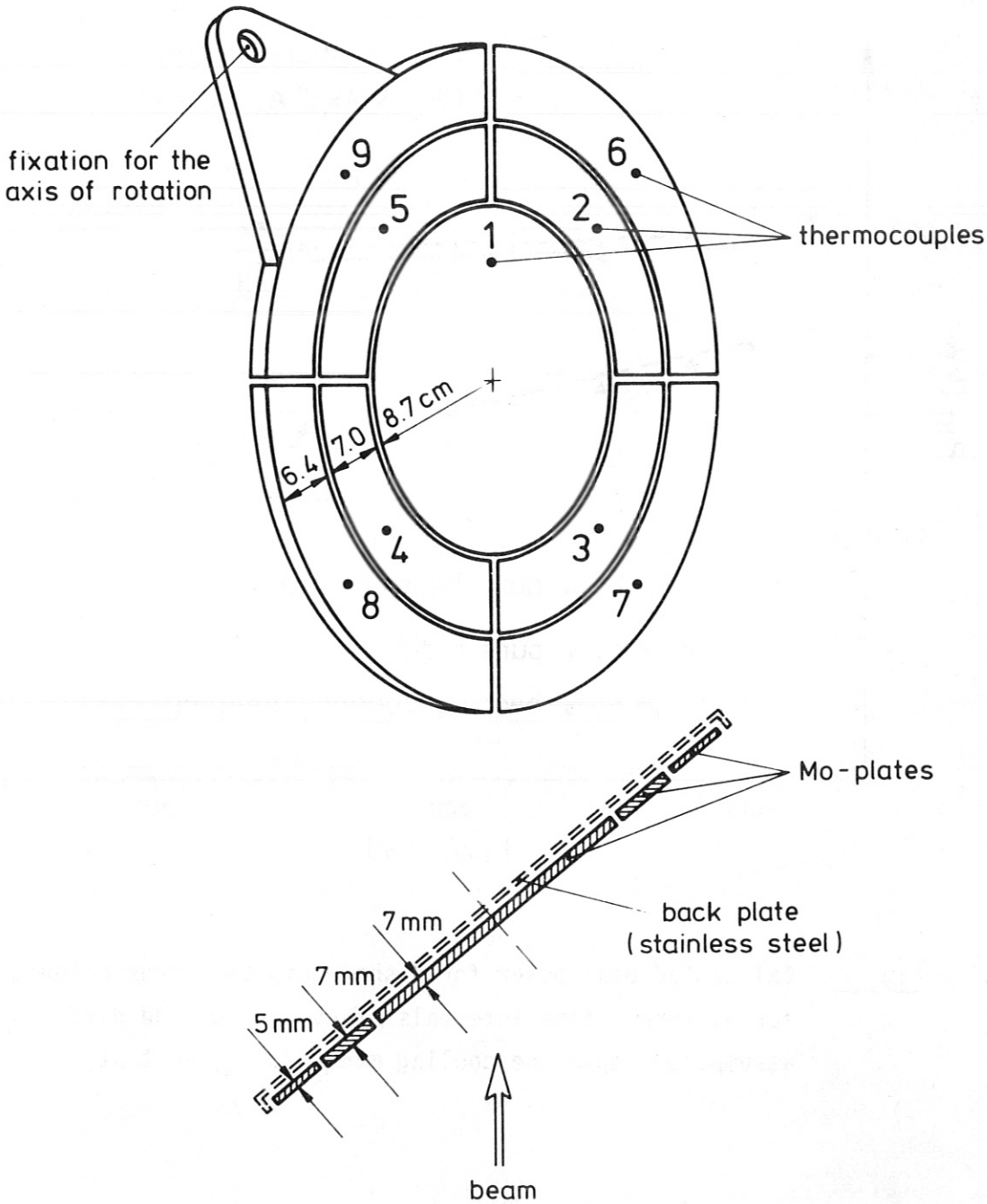

Fig. 1 Layout of the torus calorimeter

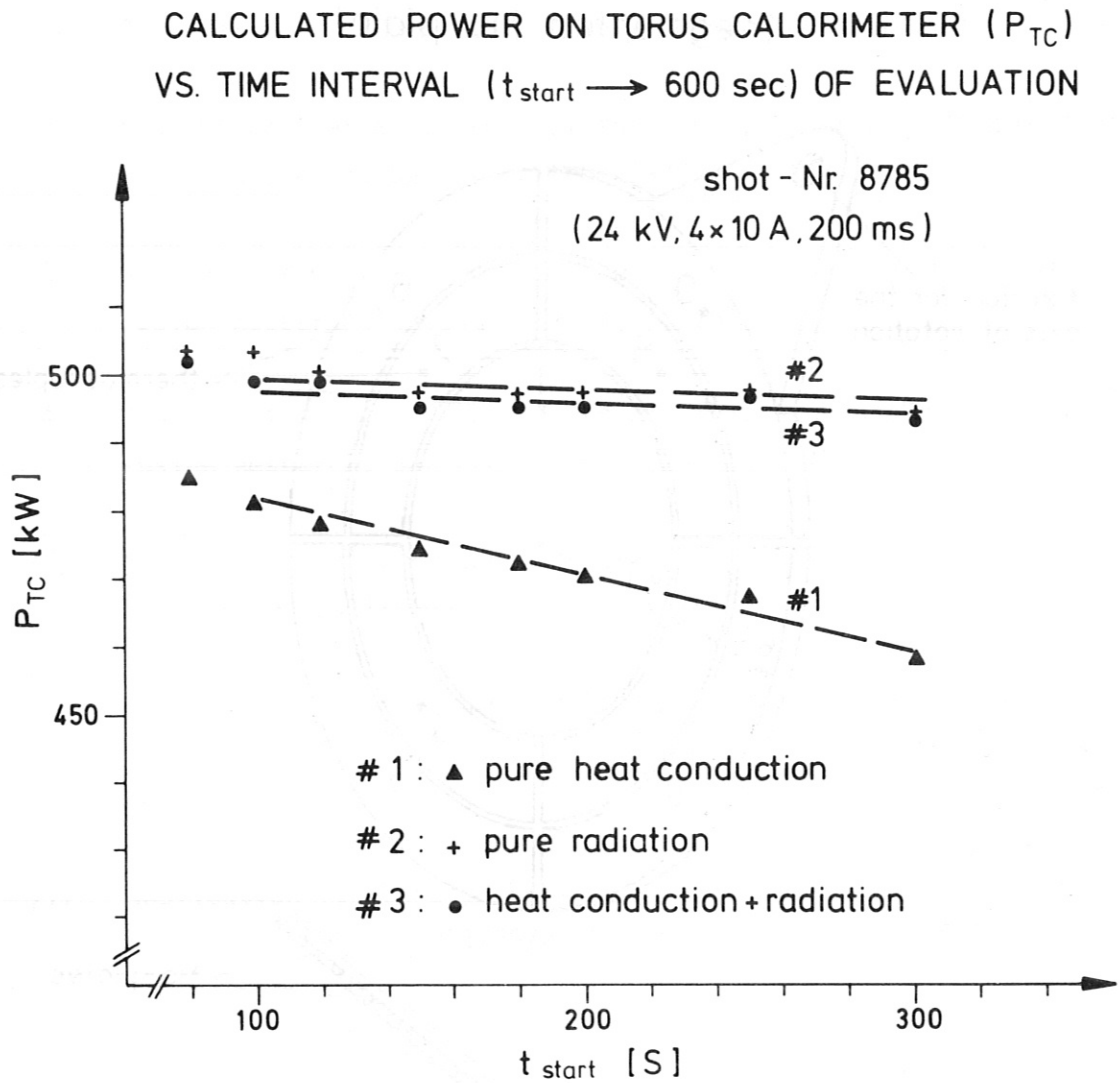

Fig. 2 Calculated beam power for a shot onto the torus calorimeter for different time intervals of evaluation and different assumptions upon the cooling mechanism (see text)